

Electrodeposition of Nickel Coating in Choline Chloride-Urea Deep Eutectic Solvent

Ping Huang^{1,2,*}, Yuan Zhang¹

¹ Panxi Science and Technology Innovation Center of Panzhihua University, Panzhihua 617000, PR China.

² Vanadium titanium school of Panzhihua University, Panzhihua 617000, PR China.

*E-mail: huangping1969@163.com

Received: 21 May 2018 / Accepted: 12 July 2018 / Published: 1 October 2018

The nickel coating is deposited onto a copper substrate in 1:2 choline chloride-urea (1:2 ChCl-urea) deep eutectic solvent (DES) containing 50 mM Ni₂O₃ at 333 K-353 K. The electrodeposition behaviour of the Ni(III) on glassy carbon and copper working electrodes have been investigated by cyclic voltammetry. The experiments results demonstrated that the reduction of Ni(III) is a diffusion controlled quasi-reversible process in ChCl-urea DES. The diffusion coefficient of Ni(III) increases from $2.24 \times 10^{-8} \text{ cm}^2 \cdot \text{s}^{-1}$ at 333K to $6.45 \times 10^{-8} \text{ cm}^2 \cdot \text{s}^{-1}$ at 353K. The effects of reaction temperature on the morphology of the nickel coatings are also examined. Smooth and dense nickel coating can be prepared on Cu substrate in Ni₂O₃-ChCl-urea solution at 343 K. The particle size of nickel grains grow up gradually with the increase of reaction temperature. The results of the XRD tests show that the obtained pure nickel coatings with face-centered cubic crystalline phase are preponderantly oriented in (111) plane.

Keywords: Nickel coating; Electrodeposition; Nickel sesquioxide; Deep eutectic solvents; Temperature

1. INTRODUCTION

Nickel has been attracted many interest as coating materials in the fields of decorative applications, magnetic applications, corrosion resistance, wear-resistant and heat-resistance coatings due to its excellent characters [1-4]. These applications require the nickel coatings with homogeneous chemical composition and small particle size. Among lots of methods [5-7], electrodeposition is confirmed to be a simple and efficient technique to prepare high-quality nickel coatings at low reaction temperature. Therefore, the electrodeposition of nickel coatings from aqueous sulfate-chloride

electrolytes has been researched extensively [8, 9]. However, the evolution of hydrogen in the deposition process will notably decrease the current efficiency and result in poor quality of the deposits [10]. To overcome the shortcoming, it is essential to find other appropriate electrolytes for the electrodeposition process. Deep eutectic solvents (DESs) have been found to be a suitable alternative for the electrodeposition of various metals, alloys and semiconductors due to their low melting points, good conductivity, nonpoisonous and biodegradable [11-13]. DESs have been applied in many fields including organic synthesis [13], material chemistry [14] and electrochemistry [14, 15], catalysis [16], dissolution and extraction process [17]. Besides, this solvent can easily dissolve a lot of metal oxides at lower temperature, such as ZnO, CuO, Cu₂O, PbO and PbO₂ [18-22]. Therefore, it opens a facile and eco-friendly method for the extraction of many metals from their oxides in almost neutral electrolyte. Ustarroz et al. [23] have obtained a highly dense distribution of nickel nanostructures on glassy carbon from NiCl₂·6H₂O by electrodeposition within a wide potential range in 1:2 ChCl-urea DES and the nanoparticles are formed by a metallic nickel core and a thin shell of nickel oxi/hydroxide. Anicai et al. [24] have reported that adherent and uniform Ni, Ni-Mo and Ni-Sn alloy coatings onto Cu substrate have been deposited from some choline chloride-based ionic liquids and characterized. The electrochemical behaviour of Ni(II) in 1-butyl-3-methylimidazolium tetrafluoroborate ionic liquid has been investigated by cyclic voltammetry at 353 K and the electrodeposition of nickel was studied at different cathodic potentials and temperatures from Ni(BF₄)₂ [10]. In addition, highly quality copper films on Ni substrate from Cu₂O and bright zinc coatings with good purity from ZnO can also be deposited in ChCl-urea DES and [Amim]Cl/urea, respectively [22, 25]. Ru et al. [26] reported that sub-micrometer lead wires on stainless steel substrate can be prepared from PbO in ChCl-urea DES and the lead wires obtained at 323K have a mean particle size of 2-4 μm in length and 1 μm in diameter.

In the present paper, the nickel coatings were firstly deposited on a copper sheet from ChCl-urea DES containing 50 mM Ni₂O₃. The electrodeposition behaviour of the Ni(III) on glassy carbon and copper working electrodes at different temperatures have been investigated preliminarily by cyclic voltammetry. The influences of reaction temperature on the morphology, composition and crystal structure of the Ni coating are also investigated.

2. EXPERIMENTAL

The raw chemicals used in this experiment were purchased commercially with analytical grade (purity > 99.90 %) from Aisinaladdin-e.com, China. Choline chloride and urea were dried under vacuum. Before use, Ni₂O₃ was dried under vacuum for 24 h at 353 K. The Ni₂O₃ raw material is irregularly granular in particle size of 2-30 μm, as shown in Fig. 1. The choline chloride and urea (mole ratio 1:2) were mixed at 353 K to prepare a homogeneous and colorless ChCl-urea DES. Then 50 mM Ni₂O₃ was added into the DES at 353 K and stirred for 12 h to form a Ni₂O₃-ChCl-urea solution.

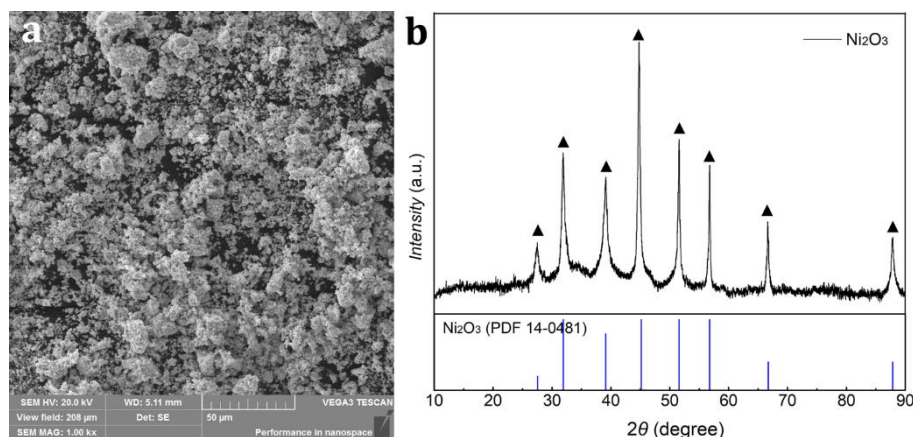


Figure 1. (a) SEM micrograph and (b) X-ray diffraction pattern of Ni₂O₃ powders.

The cyclic voltammetric measurements were performed by a CHI440C electrochemical workstation (Shanghai CH Instruments Company, China). A conventional three-electrode cell was used for these experiments. The working electrode were glass carbon (GC) and copper (Cu). An Ag wire placed in a fritted glass tube containing ChCl-urea was used as quasi-reference electrode. A platinum wire was served as counter electrode. In addition, these electrodes were polished with metallographic abrasive paper, degreased with anhydrous ethanol in an ultrasonic bath for 5 min, washed with distilled water and dried. Besides, the cyclic voltammetric measurements were conducted from negative potential to positive, and the working temperature was varied from 333 to 353 K at a scan rate of 10-100 mV·s⁻¹.

Small-scale constant potential electrolysis experiment was performed in a 50 cm³ glass cell by direct current regulated power supply (DSP-305BF model). A Cu substrate and a graphite sheet (3 cm²) were served as the cathode and anode, respectively. The interelectrode distance was 1.0 cm. Nickle coating was deposited on the Cu substrate with an effective area of 3 cm². All the electrodeposition experiments were conducted for 2 h in 50 mM Ni₂O₃+ChCl-urea at different temperatures from 333 K to 353 K. After electrolysis, the deposits were removed from the plexiglass cell and washed thoroughly with ethanol and dried.

The morphology and elemental constituents of the nickel coating were examined by SEM and EDS (XL 30 ESEM TMP model). The coatings were analyzed by XRD (D/Max-2200 model) with Cu-Kα radiation at a scan rate of 10°/min in the range of 2θ = 10–90°.

3. RESULTS AND DISCUSSION

3.1 Cyclic voltammetry

The electrochemical behaviour of Ni(III) in 50 mM Ni₂O₃+ChCl-urea DES is firstly tested and analyzed by cyclic voltammetry. Before the testing of the Ni₂O₃-ChCl-urea solution, the electrochemical behaviour of the home-made ChCl-urea DES on GC working electrode is identified at 353 K, as shown in Fig. 2. The voltammogram of the Ni₂O₃-ChCl-urea solution on GC electrode is

initiated from +0.20 V when the potential is scanned in the negative direction and reversed at -1.25 V in the positive direction. There is no significant current until the potential reaches point 'B' (-0.62 V), corresponding to the initial deposition of metallic nickel. After that, the current increases sharply to point 'C' (-1.18V) and then generates a decrease at more negative potentials which could be related to the mass transport limitation of Ni(III). The positive scanning in current is decreased and then arrive to zero at the crossover potential. The metal is always deposited at more positive position when the scan is reversed. When the scanned potential is positive than the equilibrium potential E_{eq} , i.e., at point 'B', the deposition of metal is ceased finally. The current then reaches anodic potential related to the dissolution of the metallic nickel. Therefore, the cathodic reaction can be represented as Eq. (1). Besides, the cathodic peak potential E_{pc} and anodic peak potential E_{pa} of Ni(III) are -1.18 V and +0.09 V from Fig.2, respectively. The difference in the value of $|E_{pc}-E_{pa}|$ is larger than the theoretical values of $2.3RT/nF$ (35 mV at 353 K) in reversible process, which indicates that the reduction of Ni(III) to nickel in ChCl-urea DES is a quasi-reversible process [22, 27].



Based on related references [23, 29, 30], the electrodeposition of nickel nanostructures on glassy carbon has been investigated in ChCl-urea DES containing $\text{NiCl}_2 \cdot 6\text{H}_2\text{O}$. The electrochemical tests show that the initial reduction potential of the Ni(II) is about -0.72 V (vs Ag QRE) which is similar to that in present study about -0.62 (vs Ag). According to recently reported references [12,16], due to the formation of complexes among metal oxides, urea and Cl^- ions, many metal oxides can be dissolved in ChCl-urea DES. Some literatures [20-22] state that PbO , ZnO , and Cu_2O can be coordinated with urea and Cl^- anions to form complex anion $\{[\text{Me}_x\text{O} \cdot \text{CO}(\text{NH}_2)_2] \cdot \text{Cl}^-\}^-$, where $\text{Me}=\text{Pb}$, Zn and Cu , $x=1$ and 2 . It can be deduced that complex anions $\{[\text{Ni}_2\text{O}_3 \cdot \text{CO}(\text{NH}_2)_2] \cdot \text{Cl}^-\}^-$ could be formed among Ni_2O_3 , urea and Cl^- anions. Fig. 3 shows the resonance structure of the complex anion $\{[\text{Ni}_2\text{O}_3 \cdot \text{CO}(\text{NH}_2)_2] \cdot \text{Cl}^-\}^-$ in ChCl-urea DES. Therefore, the generation of these large complex anions results in the coexistence of Ni^{3+} ion in the system.

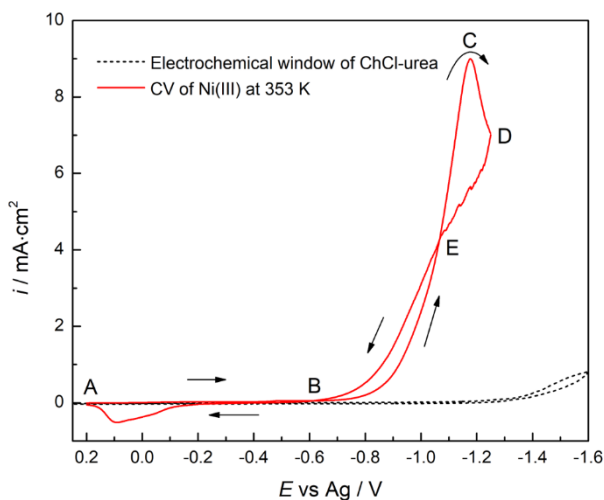


Figure 2. Cyclic voltammograms of GC electrode in 50 mM Ni_2O_3 +ChCl-urea at 353 K and $20 \text{ mV} \cdot \text{s}^{-1}$.

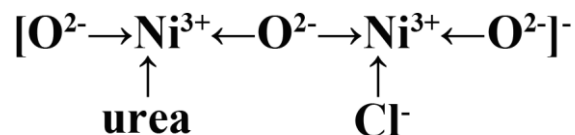


Figure 3. Resonance structure of the complex anion $\{[\text{Ni}_2\text{O}_3 \cdot \text{CO}(\text{NH}_2)_2] \cdot \text{Cl}^-\}^-$ in ChCl-urea DES.

3.2 The effect of temperature on the electrochemical behaviour of Ni(III)

The effect of temperature on the electrochemical behaviour of Ni(III) on Cu working electrode is investigated by cyclic voltammetry, as presented in Fig. 4. The cyclic voltammogram of the ChCl-urea DES using Cu electrode as working electrode is initiated from open circuit potential (-0.25 V) and the cathodic current increases obviously at potentials < -1.20 V (dash line). So, the electrochemical window of the DES is enough to support the reduction of Ni(III) to metallic nickel. The change of peak potential E_{pc} and peak current density i_{pc} at different temperatures have been summarized, as shown in Table 1. The cathodic peak potential of Ni(III) shifts positively with the increasing of temperature, indicating a promotion effect of temperature on the reduction process. In addition, the cathodic peak current increases rapidly and the influence is more obvious especially at higher temperature. It implies that the electrodeposition of nickel can be improved with increasing temperature, which is in agreement with the discussion in the literature [3]. Meanwhile, it can be noted that the initial deposition potential of the nickel is more positive at 353 K in Fig. 4. This can be attributed to the fact that a lower driving force of the cathodic reaction is required at higher temperature.

The voltammograms at different scan rates from $10 \text{ mV} \cdot \text{s}^{-1}$ to $100 \text{ mV} \cdot \text{s}^{-1}$ were recorded at different temperatures (333 K to 353 K), as shown in Fig. 5. The variation tendencies of these voltammograms are similar. With the increase of the scan rate, the cathodic peak current density i_{pc} increases and the cathodic peak potential E_{pc} shifts negatively. Because the higher the scan rate, the lower the fall in concentration of Ni(III) at the metal/solution interface, and this will lead to the increasing of current density. The plot of cathodic peak current density against square root of scan rate $v^{1/2}$ (Fig. 5f) is linear. It confirms that the reduction of Ni(III) in ChCl-urea DES is controlled by diffusion process. Therefore, the relation between the cathodic peak current density and the scan rate for an irreversible reduction reaction is given [22] by Eq. (2).

$$i_p = 0.496nFC_{\text{Ni(III)}}AD_0^{1/2} \left(\frac{\alpha n_\alpha F v}{RT} \right)^{1/2} \quad (2)$$

Where A is the electrode area in cm^2 ; $C_{\text{Ni(III)}}$ is the Ni(III) concentration in $\text{mol} \cdot \text{cm}^{-3}$; D_0 is the diffusion coefficient in $\text{cm}^2 \cdot \text{s}^{-1}$; F is the Faraday constant; R is the gas constant; n is the number of exchanged electrons; v is the potential sweep rate in $\text{V} \cdot \text{s}^{-1}$; α is the transfer coefficient; n_α is the number of electrons transferred in the rate determining step and T is the absolute temperature in K. The value αn_α can be obtained from Eq. (3).

$$\left| E_p - E_{p/2} \right| = \frac{1.857RT}{\alpha n_\alpha F} \quad (3)$$

Where $E_{p/2}$ is the half-peak potential. The diffusion coefficient, D_0 , of Ni(III) in the DES is determined to be $6.45 \times 10^{-8} \text{ cm}^2 \cdot \text{s}^{-1}$ at 353 K, which is approximate compared with the value $4.4 \times 10^{-8} \text{ cm}^2 \cdot \text{s}^{-1}$ reported in 1-butyl-3-methylimidazolium tetrafluoroborate ionic liquid containing 0.20 mol L^{-1} $\text{Ni}(\text{BF}_4)_2$ by Reddy et al. [10] and is about 10^2 times smaller in comparison to those in aqueous solutions [6].

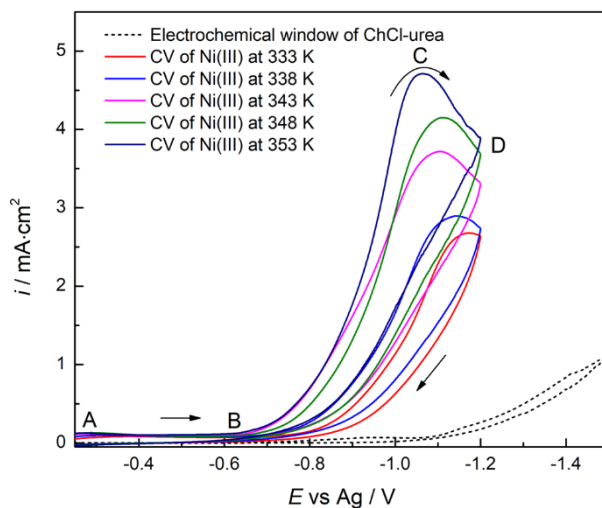


Figure 4. Cyclic voltammograms of Cu electrode in 50 mM Ni_2O_3 +ChCl-urea at different temperatures and $20 \text{ mV} \cdot \text{s}^{-1}$.

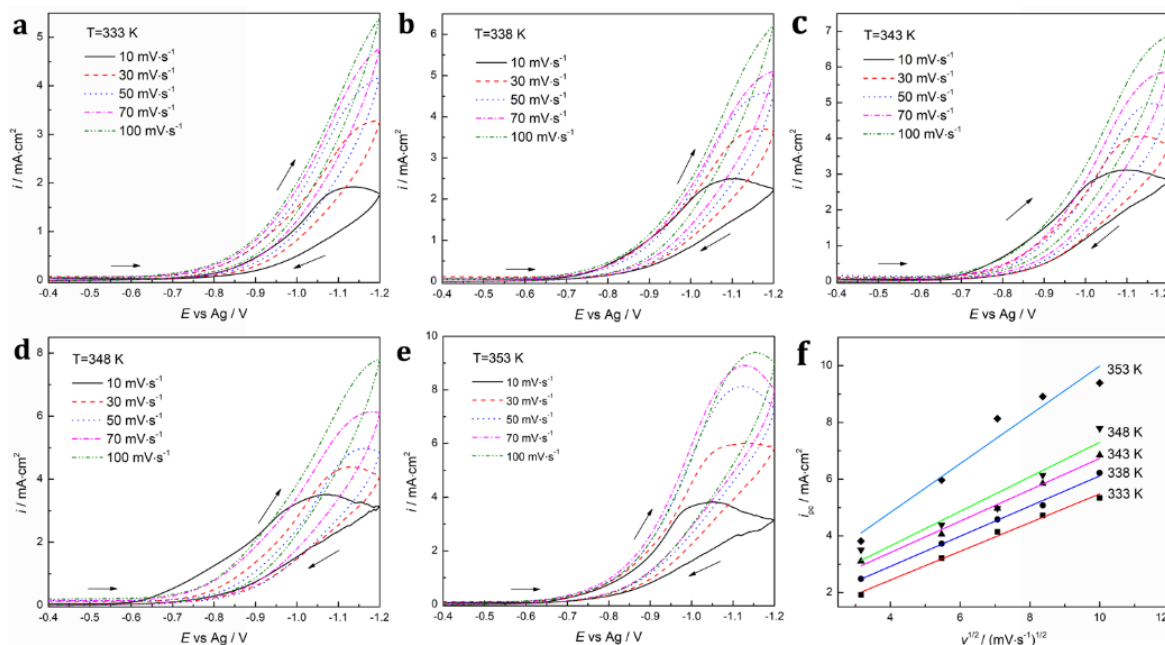


Figure 5. (a-e) Effect of scan rate on cyclic voltammograms of Cu electrode in 50 mM Ni_2O_3 +ChCl-urea, and (f) plot of cathodic peak current density i_p as a function of square root of scan rate $v^{1/2}$ at different temperatures.

This relatively low diffusion coefficient is related to the low electrical conductivity of the Ni_2O_3 -ChCl-urea solution. In addition, the diffusion coefficients at other temperatures (333 K to 348

K) are also calculated from the cyclic voltammetry curves (Fig. 5a-d) and listed in Table 1. The diffusion coefficient increases gradually from $2.24 \times 10^{-8} \text{ cm}^2 \cdot \text{s}^{-1}$ at 333K to $6.45 \times 10^{-8} \text{ cm}^2 \cdot \text{s}^{-1}$ at 353K. As well known, the reaction temperature, the properties of diffusion couples and media, the concentration of metallic ion and so on have significant effects on the diffusion coefficient of a solution. Certainly, the reaction temperature is one of the most notable factors. Based on reference [30], the viscosity of the ChCl-urea DES decreases as the increase in temperature, and it is the reverse on electrical conductivity. In this case, the migration rate of Ni(III) ions speeds up significantly and this change is reflected in the increase of diffusion coefficient.

Table 1. Effect of temperature on diffusion coefficient of Ni(III) in 50 mM Ni₂O₃+ChCl-urea.

T / K	E_{pc} / V	$i_{\text{pc}} / \text{mA} \cdot \text{cm}^{-2}$	$E_{\text{pc}} - E_{\text{pc}/2} / \text{mV}$	Slope	$D_0 \times 10^8 / \text{cm}^2 \cdot \text{s}^{-1}$
333	-1.17	2.68	150	0.50	2.24
338	-1.15	2.89	170	0.53	2.83
343	-1.11	3.72	190	0.55	3.36
348	-1.10	4.15	180	0.61	3.84
353	-1.06	4.71	120	0.86	6.45

3.3 Electrodeposition and characterization of nickel coating

The SEM micrographs of nickel coatings on Cu substrate electrodeposited in 50 mM Ni₂O₃+ChCl-urea at different temperatures and cell voltage 2.0 V for 2 h are shown in Fig. 6. As clearly can be seen from Fig. 6a and d, when the reaction temperature is 333 K, the deposit consists of homogeneous nickel grains and the surface morphology is smooth, compact and dense. It can be found in the digital image that the nickel deposit is light grey with a thin surface cover. At 343 K, light and compact nickel deposit is obtained with smooth and dense surface morphology (Fig. 6b and e). As temperature elevated to 353 K, the deposit on Cu substrate is black and spongy. Many dendrites are formed on the substrate edge so that the thickness of the deposit appears to be increased markedly. In Fig. 6f, the grooves of the substrate still can be observed and there are many clusters with larger aggregates in the particle size of 3-5 μm . This can be explained by the fast nucleation and growth rate of nickel grains at higher reaction temperature. On the one hand, the fast reaction rate leads to the formation of spongy nickel particles in the vertical direction of the Cu substrate and without time to grow in compact and dense form. On the other hand, the Ni grains are more prone to be deposited on some crystal defects, such as the protrusion of the parallel scratches, resulting in the aggravation of the grooves on the substrate. Therefore, when the reaction temperature is controlled at 343 K, smooth and dense nickel coating can be deposited in 50 mM Ni₂O₃+ChCl-urea solution. Besides, the size of the nickel grains are increased significantly, implying that the particle size of nickel grains increase gradually with reaction temperature. The reasons are presented below.

According to relative references [30], the raising of temperature benefits to the decreasing of the viscosity and the increasing of the conductivity in ChCl-urea DES. At lower reaction temperature, the migration rate of the Ni(III) ions and the cathodic reaction rate both are slow due to the higher

viscosity and lower conductivity of the DES, which will result in a inhibiting effect on the growth rate of the grains.

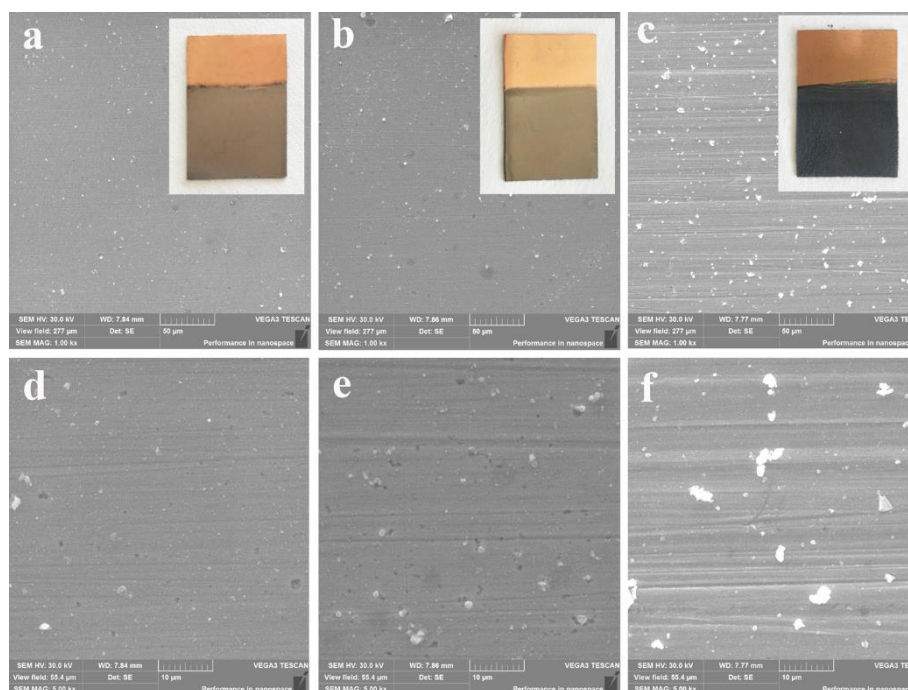


Figure 6. SEM micrographs of Ni coatings on Cu substrate electrodeposited in 50 mM $\text{Ni}_2\text{O}_3+\text{ChCl}$ -urea at different temperatures and cell voltage 2.0 V for 2 h. (a, d) 333 K, (b, e) 343 K, (c, f) 353 K. Inset: the digital images of the nickel coatings.

Thus, finer nickel grains are deposited at lower temperature. At higher reaction temperature, the ions migration rate quickens significantly so that the Ni(III) concentration on the electrode surface can be adequately provided from the bulk solution. It is consistent with the variation tendency of diffusion coefficient at different temperatures as discussed in section 3.2. This results in the increasing of the nucleation rate and grain growth rate. So, the particle size of nickel grains increase with temperature from 333 K to 353 K, resulting in the formation of dendrites at 353 K.

3.4 Composition and crystal structure analysis

The composition and crystal structure of the nickel coating deposited in 50 mM $\text{Ni}_2\text{O}_3+\text{ChCl}$ -urea DES at 343 K and cell voltage 2.0 V for 2 h, have been analyzed by EDS and XRD. The EDS pattern in Fig. 7 demonstrates that there is only nickel with a small signal from the substrate. Fig. 8 is the XRD patterns of nickel coating. The phase of the deposit is agreement with the JCPDS standard card 65-2865 and the crystal structure is face-centered-cubic structure. The nickel crystallites are predominately oriented in (111) plane. Besides, the presence of crystallites oriented in (200) and (220) planes are also observed. According to the XRD analysis through the Scherrer formula ($d=0.9\lambda/\beta\cos\theta$,

where λ is the X-ray wavelength, θ is the diffraction angle and β is the half width at half height for the diffraction peak in radians), the average sizes of crystallites are around between 53 and 97 nm.

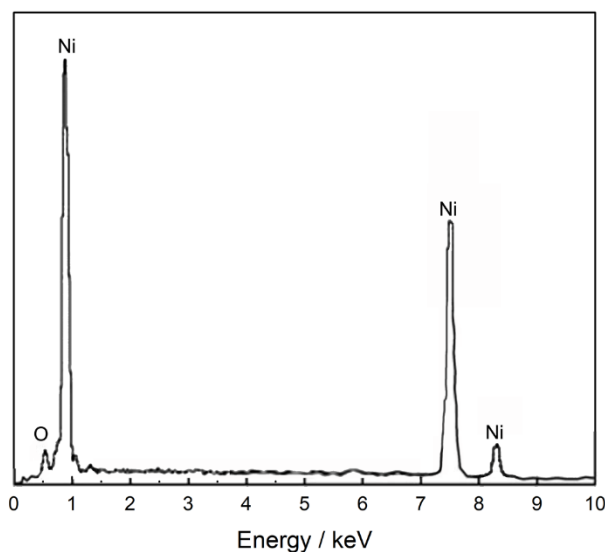


Figure 7. The EDS pattern of nickel coating on Cu substrate electrodeposited in 50 mM Ni_2O_3 +ChCl-urea at 343 K and cell voltage 2.0 V for 2 h.

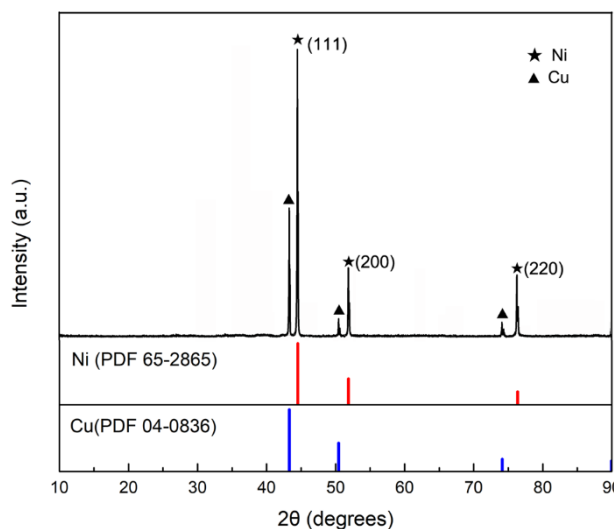


Figure 8. The XRD pattern of Ni coating on Cu substrate electrodeposited in 50 mM Ni_2O_3 +ChCl-urea at 343 K and cell voltage 2.0 V for 2 h.

4. CONCLUSIONS

(1) Light and compact Ni coatings are prepared by electrodeposition on Cu sheet using Ni_2O_3 as raw materials in ChCl-urea DES at 343 K.

(2) The reduction of Ni(III) in ChCl-urea DES is a diffusion controlled quasi-reversible process. The initial deposition potential of the nickel is more positive at high temperatures and the diffusion coefficient of Ni(III) increases gradually from $2.24 \times 10^{-8} \text{ cm}^2 \cdot \text{s}^{-1}$ at 333K to $6.45 \times 10^{-8} \text{ cm}^2 \cdot \text{s}^{-1}$ at 353K.

(3) Smooth and dense Ni coating is prepared on Cu substrate in Ni_2O_3 -ChCl-urea solution at 343 K. The particle size of Ni grains grow up progressively with the increase of the reaction temperature.

References

1. J.K. Dennis and T.E. Such, Nickel and Chromium Plating, Crc Press, (1993) Florida, American.
2. R.A. Shakoor, R. Kahraman, U.S. Waware, Y. Wang, and W. Gao, *Int. J. Electrochem. Sci.*, 9 (2014) 5520.
3. Y. Yang, C. Xu, Y. Hua, J. Li, F. Li and Y.F. Jie, *Int. J. Electrochem. Sci.*, 10 (2015) 1979.
4. Y.H. Ahmad, A.M.A. Mohamed, T.D. Golden, and N. D'Souza, *Int. J. Electrochem. Sci.*, 9 (2014) 6438.
5. L. Aymard, B. Dumont and G. Viau, *J. Alloy. Compd.*, 242 (1996) 108.
6. B.N. Mondal, A. Basumallick and P.P. Chattopadhyay, *J. Alloy. Compd.*, 457 (2008) 10.
7. S.T. Aruna, C.N. Bindu, V.E. Selvi, V.K.W. Grips and K.S. Rajam, *Surf. Coat. Tech.*, 200 (2006) 6871.
8. R. Oriňáková, A. Turoňová, D. Kladeková, M. Gálová and R.M. Smith, *J. Appl. Electrochem.*, 36 (2006) 957.
9. E. Moti, M.H. Shariat and M.E. Bahrololoom, *Mater. Chem. Phys.*, 111 (2008) 469.
10. M. Li, Z. Wang and R.G. Reddy, *J. Electrochem. Soc.*, 161 (2014) D150.
11. Z. Su, *Int. J. Electrochem. Sci.*, 11 (2016) 3325.
12. A.P. Abbott, A. Ballantyne, R.C. Harris, J.A. Juma and K.S. Ryder, *Electrochim. Acta*, 176 (2015) 718.
13. A.P. Abbott, A. Ballantyne, R.C. Harris, J.A. Juma and K.S. Ryder, *Phys. Chem. Chem. Phys.*, 19 (2017) 3219.
14. S.M. Gengan Saravanan, *Int. J. Electrochem. Sci.*, 6 (2011) 1468-1478.
15. J. Ru, Y. Hua, C. Xu, J. Li, Y. Li, D. Wang, C. Qi and Y. Jie, *Appl. Surf. Sci.*, 335 (2015) 153.
16. P.M. Pawar, K.J. Jarag and G.S. Shankarling, *Green Chem.*, 13 (2011) 2130.
17. A.P. Abbott, P.M. Cullis, M.J. Gibson, R.C. Harris and E. Raven, *Green Chem.*, 9 (2007) 868.
18. A.P. Abbott, G. Capper, D.L. Davies and P. Shikotra, *Min. Proc. Ext. Met.*, 115 (2006) 15.
19. Y. Zheng, K. Dong, Q. Wang, S. Zhang, Q. Zhang and X. Lu, *Sci. China Chem.*, 55 (2012) 1587.
20. H. Yang and R.G. Reddy, *Electrochim. Acta*, 178 (2015) 617.
21. J. Ru, Y. Hua and D. Wang, *J. Electrochem. Soc.*, 164 (2017) D143.
22. T. Tsuda, L.E. Boyd, S. Kuwabata and C.L. Hussey, *J. Electrochem. Soc.*, 157 (2010) F96.
23. E.A.M. Cherigui, K. Sentosun, P. Bouckenooge, H. Vanrompay, S. Bals, H. Terryn and J. Ustarroz, *J. Phys. Chem. C* 121 (2017) 9337.
24. A. Florea, L. Anicai, S. Costovici, F. Golgovici, T. Visan, *Surf. Interface Anal.*, 42 (2010) 1271.
25. Z. Yong, K. Dong, W. Qian, S.J. Zhang, Q.Q. Zhang and X.M. Lu, *Sci. China Chem.*, 55 (2012) 1587.
26. J. Ru, Y. Hua, C. Xu, J. Li, Y. Li, D. Wang, K. Gong and Z. Zhou, *Adv. Powder Technol.*, 26 (2015) 91.
27. A.J. Bard, L.R. Faulkner, A. Bard and L. Faulkner, *Electrochemical Methods: Fundamentals and Applications*, 2nd edn, Wiley, (2001) New York, American.
28. J. Aldana-González, M. Romero-Romo, J. Robles-Peralta, P. Morales-Gil, E. Palacios-González,

- M.T. Ramírez-Silva, J. Mostany and M. Palomar-Pardavé, *Electrochim. Acta*, 276 (2018) 417.
29. H. Guo, Z. Huang, Y. Zheng, and S. Weng, *Int. J. Electrochem. Sci.*, 10 (2015) 10703.
30. Y.L. Zhu, Y. Kozuma, Y. Katayama and T. Miura, *Electrochim. Acta*, 54 (2009) 7502.

© 2018 The Authors. Published by ESG (www.electrochemsci.org). This article is an open access article distributed under the terms and conditions of the Creative Commons Attribution license (<http://creativecommons.org/licenses/by/4.0/>).